ECONOMIC OPTIMIZATION AND GLOBAL SENSITIVITY ANALYSIS OF POWER-TO-HEAT SYSTEMS IN A SMALL DISTRICT HEATING NETWORK: A CASE STUDY

Eero Inkeri[1]*, Jussi Saari[1], Konstantin Zaynetdinov[1], Mariia Kozlova[2], Päivi Sikiö[1], Tero Tynjälä[1]

[1]LUT University, School of Energy Systems, Lappeenranta, Finland
[2] LUT University, Business School, Lappeenranta, Finland

*Corresponding Author: eero.inkeri@lut.fi

ABSTRACT

A novel method is proposed and demonstrated for the optimization of the operation of power-to-heat systems with energy storage. It is based on semi-brute force for operation optimization and heuristic optimization for the unit capacities to minimize the levelized cost of produced heat. The method enables easy implementation of nonlinear features, such as lookup tables. A case study including an air-source heat pump and electric boiler is used to demonstrate both the method and the benefits of power-to-heat. Local climate conditions and hourly electricity prices of Finland are used. A global sensitivity analysis is conducted for the various cost parameters. The model turned out to be viable for business case analysis. The results indicate a strong potential for electric boiler combined with heat storage. The air-source heat pump was rarely found in the optimal solution, and the capacities were mainly low, reflecting the limitations of air as a heat source in cold climates. Higher capacities were found for biomass boiler, but it, too, was optimized out of the production palette in over half of the solutions.

1 INTRODUCTION

Heating is responsible for 40% of global CO_2 emissions (IEA, 2019). Heat is used in industrial processes and buildings (space and water heating). Electrification has the potential to reduce fossil fuel use and CO_2 emissions (IEA, 2019), provided that the electricity has low CO_2 emissions. Heat pumps can be used to improve the performance of electric heat production further (David *et al.*, 2017).

If electricity is largely produced by variable renewable energy (VRE), e.g., wind and solar, energy systems will need to become more flexible (Rinaldi *et al.*, 2022). As space heating demand follows ambient temperature, electrification of heating may also increase peak loads (Hutty *et al.*, 2020). A high VRE share can be expected to increase price variation (Wen *et al.*, 2022). Load and price peaks support the use of thermal energy storage (TES) to decouple energy production and consumption temporally. Avoiding moments of high prices is beneficial for cost-effectiveness, and lowering peak loads can decrease the investments in both the electricity grid and dispatchable production capacity.

This study has two goals: presenting a novel way to optimize the operation and design of a system with a TES and demonstrating the economic benefits of heat production with an electric boiler, heat pump, and TES. The methodology consists of two optimization layers: component sizing optimization, and system operation optimization at one-hour time steps. Wu & Ma (2021) have conducted a review of optimization methods for electricity battery storage, which is analogous to TES. Traditional methods such as linear programming (LP), and mixed-integer linear and non-linear programming (MILP and MINLP) are extensively studied, but the strict structure of the constraints may limit the models and often require simplifications or linearization (Tarragona *et al.*, 2021; Montero *et al.*, 2022). Studies often use simple models: TES heat losses may be neglected (Zhang *et al.*, 2022; Dorotić *et al.*, 2019) or estimated with a simple efficiency (Fischer *et al.*, 2016), and heat pump coefficient of performance (COP) estimation is often simplified (Tarragona *et al.*, 2022; Krützfeldt *et al*., 2021).

https://doi.org/10.52202/077185-0047

Metaheuristics such as particle swarm optimization (PSO), and genetic algorithm (GA) have more freedom in model formulation, permitting e.g., a detailed solar collectors and TES model described with partial differential equations to be optimized with PSO (Immonen & Powell, 2022). The drawbacks of metaheuristics include their computational load, and lack of convergence proof (Li *et al.*, 2014; Siddiqui *et al.*, 2021). Dynamic optimization (DO) has also been applied to TES operation (Siddiqui *et al.*, 2021). However, the model preparation may be demanding (Jain & Singh, 2003). The hypothesis of this study is that (i) it is easy to include non-linear features and detailed models in an explicit time-marching solver, (ii) rule-based DO can serve as a semi-brute-force method, the rules limiting the number of options.

The capacity optimization is performed using the CS3 cuckoo search metaheuristic (Saari *et al.*, 2022). For improved performance, a modified Hooke-Jeeves search is implemented for terminal convergence. Finally, a global sensitivity analysis is carried out by the SimDec method (Tarantola *et al.*, 2024).

The main benefit of the proposed method is the ability to use complex models in a time-marching solver. This enables easy implementation of accurate component models without linearization. The method is demonstrated with a case study, in which heat for a small district heat (DH) network is supplied by a system consisting of wood- and oil-fired boilers, an electric boiler, an air-source heat pump, and a TES. The optimization objective is minimizing the levelized cost of heat. Two cases are studied: in one there is an existing wood boiler, in the other, the wood boiler capacity is also a decision variable.

2 METHODS

2.1 The studied case

The proposed method and the potential of electrified heating and thermal energy storages are demonstrated with a case study, a small DH system (Fig. 1). The operation and capacities of the available heat sources are optimized, to minimize the cost of produced heat. The heat demand data is obtained from a Finnish energy company operating several DH networks in Finland. The maximum heat rate and annual heat demands are 6.5 MW and 18.5 GWh, respectively.

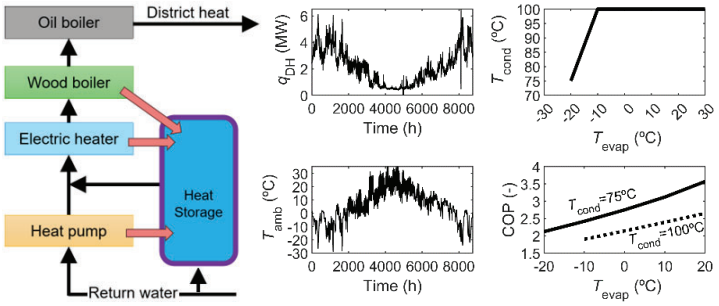

Figure 1: The case, district heat demand (q_{DH}), ambient temperature (T_{amb}), and the performance of the heat pump for different evaporation (T_{evap}) and condensing (T_{cond}) temperatures.

The developed model consists of two parts: (1) the core model contains an explicit time-marching energy and mass balance, and the optimization of the system operation, (2) the outer layer minimizes the levelized cost of heat by optimizing unit capacities. The model is built in a MATLAB environment. The objective function of the outer layer optimization is levelized cost of heat (LCOH) minimization,

$$LCOH = \frac{\frac{i(1+i)^{lt}}{(1+i)^{lt}-1} CAPEX + OPEX}{E_{DH}}, \quad (1)$$

where the cost of production is obtained from the capital expenditure (CAPEX) annualized with the capital recovery factor defined through lifetime *lt* and interest *i*, and operating expenditure OPEX. The costs are divided by the produced energy for district heat E_{DH}. The model includes a water tank type of thermal energy storage (TES), and four heat sources: an air-source heat pump (HP), an electric boiler

https://doi.org/10.52202/077185-0047

(EB), a wood chip-fired biomass boiler (BB), and a light fuel oil boiler (LFOB). Quasi-steady operation with a one-hour time step is considered. Constant heat capacity c_p is used for water.

2.2 Thermal Energy Storage

The TES charge rate q_{charge} is solved from energy balance with heat production rates q and demand $q_{DH,}$

$$q_{\mathrm{charge}} = q_{\mathrm{HP}} + q_{\mathrm{EB}} + q_{\mathrm{BB}} + q_{\mathrm{LFOB}} - q_{\mathrm{DH}}, \tag{2}$$

Negative q_{charge} means discharge. The TES is modelled as a perfectly stratified cylinder with constant-temperature hot and cold parts, and 15 W/m^2 heat loss (Koskelainen *et al.*, 2006). The state of charge (SOC) is determined at each time step by the difference between the TES and DH return temperatures,

$$SOC = m_{\mathrm{TES}}\, c_{\mathrm{p}}\left(T_{\mathrm{TES}} - T_{\mathrm{DH,in}}\right), \tag{3}$$

The temperature of TES hot part changes during charge, as the charging water temperature may differ from the TES temperature. The charging temperature T_{charge} is the DH supply T. DH return water is mixed with the TES the cold water. Hot temperature at moment n+1 is obtained from

$$T_{\mathrm{TES}}^{n+1} = \frac{c_{\mathrm{p}} m_{\mathrm{TES}}^{n} T_{\mathrm{TES}}^{n} + c_{\mathrm{p}} m_{\mathrm{charge}} T_{\mathrm{charge}}}{c_{\mathrm{p}} m_{\mathrm{TES}}^{n} + c_{\mathrm{p}} m_{\mathrm{charge}}} - \frac{q_{\mathrm{loss}} \Delta t}{c_{\mathrm{p}} m_{\mathrm{TES}}^{n}}, \tag{4}$$

$$m_{\mathrm{charge}} = \frac{q_{\mathrm{charge}} \Delta t}{c_{\mathrm{p}}\left(T_{\mathrm{DH,supply}} - T_{\mathrm{DH,return}}\right)}. \tag{5}$$

During discharge, hot water is drawn from the TES and supplied to the DH network. Other sources may be used simultaneously to cover part of the demand. The required discharge mass is solved from

$$m_{\mathrm{charge}} = \frac{\dot{m}_{\mathrm{DH}} c_{\mathrm{p}}\left(T_{\mathrm{DH,supply}} - T_{\mathrm{DH,return}}\right) - q_{\mathrm{HP}} - q_{\mathrm{EB}} - q_{\mathrm{BB}} - q_{\mathrm{LFOB}}}{c_{\mathrm{p}}\left(T_{\mathrm{TES}} - T_{\mathrm{DH,return}}\right)} \Delta t, \tag{6}$$

where the time step Δt is one hour. Limited TES charge or temperature may limit the ability to cover the heat demand from the TES. In such case, discharge is mixed with remaining return water resulting in a mixing temperature T_{mix}, Eq.(7) and initial estimate for supply temperature T_{supply}^{0}, Eq.(8)

$$T_{\mathrm{mix}} = \frac{\dot{m}_{\mathrm{DH}} c_{\mathrm{p}} T_{\mathrm{TES}} + (\dot{m}_{\mathrm{DH}} - \dot{m}_{\mathrm{TES}}) T_{\mathrm{DH,return}}}{\dot{m}_{\mathrm{DH}} c_{\mathrm{p}}}, \tag{7}$$

$$T_{\mathrm{supply}}^{0} = \frac{\dot{m}_{\mathrm{DH}} c_{\mathrm{p}} T_{\mathrm{mix}} + q_{\mathrm{HP}} + q_{\mathrm{EB}} + q_{\mathrm{BB}} + q_{\mathrm{LFOB}}}{\dot{m}_{\mathrm{DH}} c_{\mathrm{p}}}. \tag{8}$$

If T_{supply}^{0} is insufficient, the discharge mass or temperature was insufficient, and additional heat q_{add} is needed from the available sources (HP, EB, BB, LFOB), Eq.(9), and discharge must be re-calculated, Eq.(10):

$$q_{\mathrm{add}} = \dot{m}_{\mathrm{DH}} c_{\mathrm{p}}\left(T_{\mathrm{DH,supply}} - T_{\mathrm{supply}}^{0}\right), \tag{9}$$

$$q_{\mathrm{charge}} = q_{\mathrm{HP}} + q_{\mathrm{EB}} + q_{\mathrm{BB}} + q_{\mathrm{LFOB}} + q_{\mathrm{add}} - q_{\mathrm{DH}}. \tag{10}$$

2.3 Heat production

The air-source heat pump (HP) uses a centrifugal compressor, and pentane as work fluid. The coefficient of performance (COP) is determined by a model described in Jaatinen-Värri *et al.* (2024) at -20 °C < $T_{evaporation}$ < 20 °C and 75 °C < $T_{condensation}$ < 100 °C (Fig.1), with additional constraint of 20% minimum load. Temperature difference of 10 °C is assumed between the ambient and evaporator, due to the heat exchangers of the heat collector system. Electric and LFO boilers have no limitations on minimum load. The biomass boiler minimum load is 15%; minimum operating and idle time were varied in a sensitivity analysis.

2.4 Optimization of the system operation

Optimizing the system operation is based on a 24-hour semi-brute force horizon, with the number of possible options reduced by rules. The method uses for-loops going through different price limits to operate the system while solving the energy balance explicitly. Algorithm 1 presents the method in pseudocode. The 24-hour optimization is repeated through the simulation. The initial state of an

https://doi.org/10.52202/077185-0047

optimization comes from the last step of the previous. Historical data is used for electricity prices and heat demands. Charging TES during lowest-price hours is assumed the best option. From no charging to charging at every hour, there are thus t_{opt}+1 = 25 charging options. Discharge is always allocated for the hours of the most expensive electricity. An example of all options for one optimization horizon is shown in Fig.3.

During charging, heat production q_{prod} is constrained by TES free capacity, heat demand during the rest of the optimization period, and production unit capacities. Three possible combinations are available for TES charging: (1) HP+EB, (2) HP+BB, or (3) BB. Options (1) and (2) are possible when the electricity price is below the threshold. The choice of (1) or (2) is based on the following rules:

- Heat pump is the primary source.
- If the heat pump cannot provide the full heat or temperature, EB or BB is used as a supplementary heat source; choice is based on opex.
- If BB is shut down, EB is used as a supplementary heat source.

Algorithm 1. Main algorithm for one optimization horizon t_{opt}.

C_{el} = hourly electricity prices
$C_{el,sorted}$ = sorted hourly electricity prices
for i = from 1 to t_{opt} + 1 **do**
for h = from 1 to 24 **do**
if $C_{el}(h) < C_{el,sorted}(i)$ **then**
Charge with HP+EB or HP+BB
elseif peak demand between h and 24 exceeds BB capacity **then**
Charge with BB
else
No charging
if discharge allowed **then**
Try to provide heat from TES
end if
end if
Cover missing heat with HP, EB, BB, and LFOB
Update state of charge of TES
end for
end for

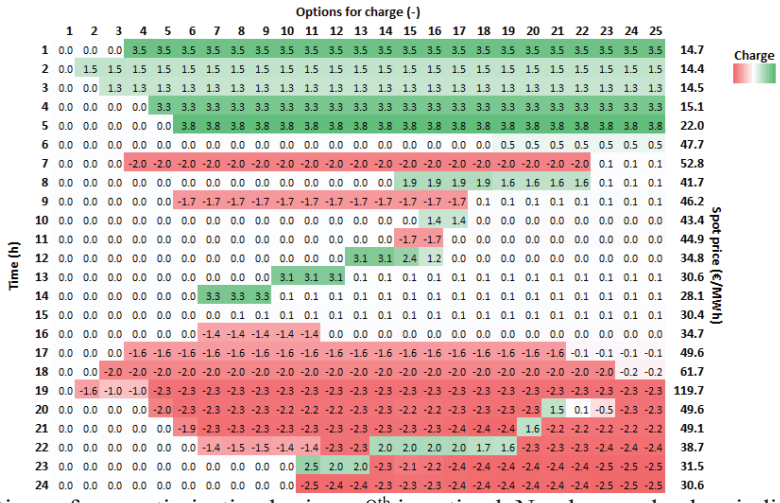

Figure 3: Options of one optimization horizon; 8th is optimal. Numbers and colors indicate the charge and discharge of TES.

https://doi.org/10.52202/077185-0047

If the electricity price exceeds the threshold, TES can still be charged with BB alone, if the peak heat demand during the rest of the optimization period exceeds BB capacity. TES discharge is tried if allowed. There is one discharge option per charging option (Fig.3). The rules are:

- Number of hours that TES can cover heat demand: $n_{\text{discharge}} = SOC/q_{\text{DH}}$
- Allocate $n_{\text{discharge}}$ for the most expensive hours of the optimization horizon.
- Check if TES can provide the required discharge, Eq.(2)–(8). If not, calculate the additional heat required, Eq.(9)–(10).

If any heat demand remains after charge/discharge, the heat sources (HP, EB, BB, LFOB) can be used to cover the additional demand q_{add} if there is capacity left. The rules for heat sources selection are:

- Heat pump is the primary source.
- If the heat pump cannot provide the full heat or temperature (Fig.2), boilers are used.
- Selection between EB, BB, and OB is done by specific opex and available capacity

2.5 Capacity optimization

The heat production unit capacities were optimized with the CS3/rand/1/bin cuckoo search (Saari *et al.*, 2022). The CS3 is a population-based method based on differential mutation and Lévy-distributed random walks. The CS3 typically finds the region of the solution relatively fast, spending most of the run refining it. To improve speed, a deterministic direct method was used for terminal convergence. Hooke-Jeeves (HJ) pattern search (Hooke & Jeeves, 1961) is a well-known method, but it suffers from a limited ability to search outside of the variable axes: such moves can only be sums of successful single-axis moves. To alleviate this, the possibility of diagonal moves was added (Alg.2).

Algorithm 2. *Modified Hooke-Jeeves algorithm to minimize* $f(\mathbf{x})$

```
begin
    n ← 0; set initial step length vector Δx_n ← (Δx_n,1, Δx_n,2, …, Δx_n,D)
    while number of function valuations < maximum and there exists Δx_n,d > minimum threshold
        f_n ← f(x_n); n ← n+1
        for all i = 1, …, D do                                  // try moves in direction of each axis
            attempt moves by +/- Δx_n,i ;update x_n if succesful
        end for
        if x_n = x_n−1                                          // if no move was accepted
            reduce step size: Δx_n+1 ← ε Δx_n
            x_n = diagonal_exploration(x_n, Δx_n)
        else                                                    // otherwise try pattern move
            attempt further pattern moves by the sum vector of all successful moves, until failure
        end if
    end while
end
begin function diagonal_exploration(x_n, Δx_n)
    for all i = 1, …, D-1 do
        for all j = i+1, …, D do
            attempt all 4 possible diagonal moves possible with ±Δx_n,I ± Δx_n,j
            if x_k,i+1 = x_k,i and j < D                        // if two-axis moves fail, try three-axis moves
                for all k = j+1, …, D do
                    attempt all 8 possible diagonal moves possible with ±Δx_n,i ± Δx_n,j ± Δx_n,k
                end for
            end if
        end for
    end for
    if x_k,i+1 ≠ x_k,i
        attempt pattern moves until failure
    end if
end function
```


https://doi.org/10.52202/077185-0047

2.6 Global sensitivity analysis

Global sensitivity analysis is important for any analysing systems with uncertainties (Saltelli *et al.*, 2019). One recent technique is a hybrid uncertainty-sensitivity analysis approach, Simulation Decomposition or SimDec (Tarantola et al., 2024). SimDec decomposes the distribution of the output (target variable) by the multivariable scenarios, formed out of the most influential input variables (Kozlova & Yeomans, 2022), where the influence of inputs is defined by variance-based sensitivity indices (Kozlova *et al.*, 2023). The procedure reveals how different output ranges are achieved, and what parameter interactions affect the output (Kozlova *et al.*, 2024). For each case, two forms of visualization, stacked histogram and box plots, produced with the same decomposition, are presented. The histogram highlights the output distribution, while the box plot indicates the extent of scenarios.

Many central parameters of the studied case, particularly energy prices but also equipment costs, have considerable uncertainties, and interactions between the uncertain parameters are also likely. The optimization was thus carried out in conjunction with a global sensitivity analysis.

3 RESULTS

The results were obtained through 1024 Monte Carlo simulation runs, where each simulation run is an optimization with randomized values of uncertain parameters. In each case, 8% interest and 20-year lifetime, were considered. Annual operating costs of all units were estimated at 3% of capex (fixed) plus 3 €/MWh (variable). For electricity, the hourly energy price fluctuations were based on hourly historical data from 2020 (Nord Pool, 2022), varied by correction factors in a sensitivity analysis. To this was added a fixed 0.6 €/MWh tax according to Finnish tax class II and transmission costs of 13.6 and 30.6 €/MWh for night and day times, respectively (Lappeenrannan Energia, 2022).

The variables subjected to sensitivity analysis are listed in Table 1. In each run, the electricity hourly prices were adjusted up or down by a constant factor of 0.5-2.0. The median was kept at 1.0 by dividing or multiplying at equal probability with a uniform-distributed random variable between 1 and 2; the mean value will thus be somewhat greater than the median. All other prices are uniform-distributed random numbers between the minimum and maximum.

Two cases were studied: (1) pre-existing biomass boiler, (2) clean sheet case. The first one serves as a retrofit for a typical small-scale DH system, and the latter illustrates how a new, greenfield system could be designed.

Table 1: Energy and grid connection costs.

	Variable	Min	Median	Max	References
Boilers	Light fuel oil, €/MWh	70	160	250	(Statistics Finland, 2024)
	Wood chips, €/MWh	20	35	50	(Bioenergia, 2023)
	Minimum wood boiler oper./idle time, h	6	12	18	This study
Electr.	Electricity spot price multiplier, -	0.5	1.0	2.0	This study
	Share of electricity from the spot market, %	0	50	100	This study
	Peak power cost, k€/MW/month	1.0	3.0	5.0	(Lappeenrannan Energia, 2022)
CAPEX	Heat pump CAPEX, €/kW	630	900	1170	(Pieper *et al*., 2018)
	Electric boiler CAPEX, €/kW	35	50	65	(Trevisan *et al*., 2022)
	Thermal energy storage CAPEX, €/MWh	1400	2000	2600	(Dahash *et al*., 2021)
	Biomass boiler CAPEX, €/MW	700	1000	1300	(Dahl *et al.*, 2019)

3.1 Pre-existing biomass boiler

The electricity price and wood fuel price have the greatest influence on LCOH, as seen in Fig.4. At the lower electricity prices, the wood boiler is used less. Its cost affects the LCOH only moderately, as indicated by the fairly slight shift to the right with the lighter shades of the red- and yellow-colored low- and medium-price electricity scenarios. At the high electricity prices, wood use increases, and therefore also the influence of its cost on LCOH becomes significantly more, indicated by the clearly increased spread of shades of blue.

https://doi.org/10.52202/077185-0047

The decomposition for heat pump (HP) capacity, indicated as compressor power consumption, is shown in Fig.5. In more than half of the optimization runs, no HP was installed. When one was included, it was typically under combinations of low HP specific cost, and expensive wood chips (a light red scenario in Fig.5), but even then, the capacity was comparatively small.

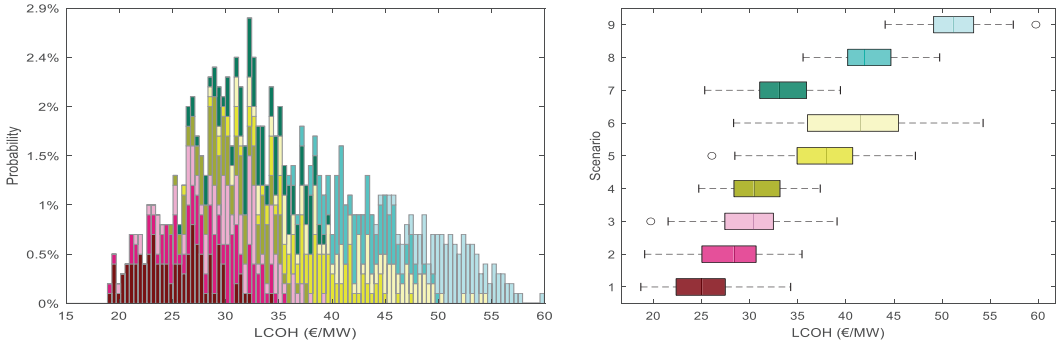

Color	Electricity price	Price of wood chips	LCOH (€/MW)			Share of data
			min	mean	max	
	low	low	18.7	25.0	34.3	11 %
		medium	19.1	28.0	35.4	11 %
		high	19.7	30.1	39.1	11 %
	medium	low	24.7	30.6	37.3	11 %
		medium	26.1	37.5	47.2	11 %
		high	28.3	41.0	54.3	11 %
	high	low	25.3	33.2	39.4	11 %
		medium	35.6	42.3	49.7	12 %
		high	44.1	51.2	59.7	11 %

Figure 4: Levelized cost of heat (LCOH).

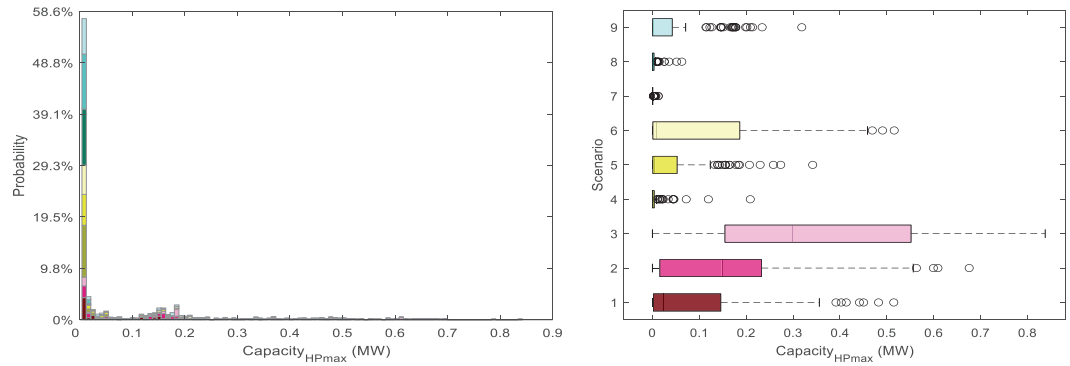

Color	HP CAPEX	Price of wood chips	HP capacity [MW]			Share of data
			min	mean	max	
	low	low	0.00	0.09	0.51	11 %
		medium	0.00	0.17	0.68	11 %
		high	0.00	0.33	0.84	11 %
	medium	low	0.00	0.01	0.21	12 %
		medium	0.00	0.05	0.34	11 %
		high	0.00	0.11	0.52	11 %
	high	low	0.00	0.00	0.01	11 %
		medium	0.00	0.00	0.06	12 %
		high	0.00	0.04	0.32	11 %

Figure 5: Heat pump (HP) capacity, as design-point compressor electric power consumption.

https://doi.org/10.52202/077185-0047

Fig.6 shows the decomposition of electric boiler sizing. The electric boilers were sized much larger – only in ca.10% of the cases less than 0.5 MW, and at the high end, nearly 6 MW was sometimes installed, amounting to almost 90% of the system's maximum heat rate. Unsurprisingly, the prices of electricity and the cost for grid connection peak power were the most important variables explaining the electric boiler sizing. The distribution of capacities indicates a multi-modal problem.

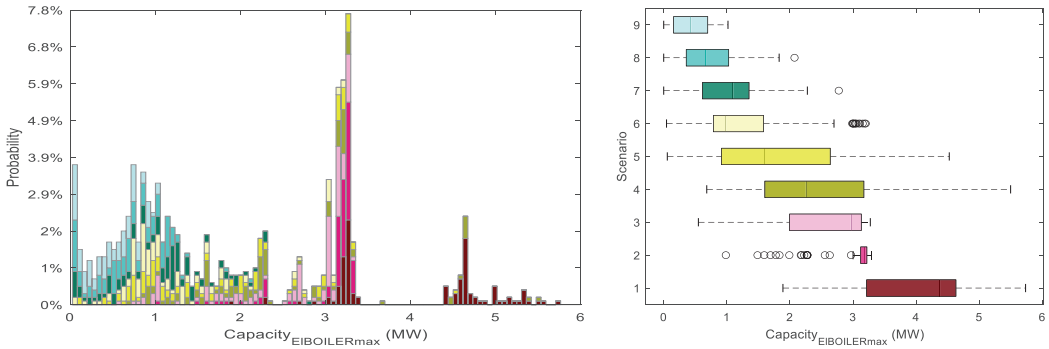

Color	Electricity price	Grid connection peak power cost	Electric boiler capacity (MWh) min	mean	max	Share of data
	low	low	1.9	4.0	5.7	11 %
		medium	1.0	3.0	3.3	10 %
		high	0.5	2.5	3.3	12 %
	medium	low	0.7	2.5	5.5	11 %
		medium	0.1	1.8	4.5	11 %
		high	0.0	1.3	3.2	11 %
	high	low	0.0	1.0	2.8	11 %
		medium	0.0	0.7	2.1	12 %
		high	0.0	0.4	1.0	10 %

Figure 6: Electric boiler (EB) capacity.

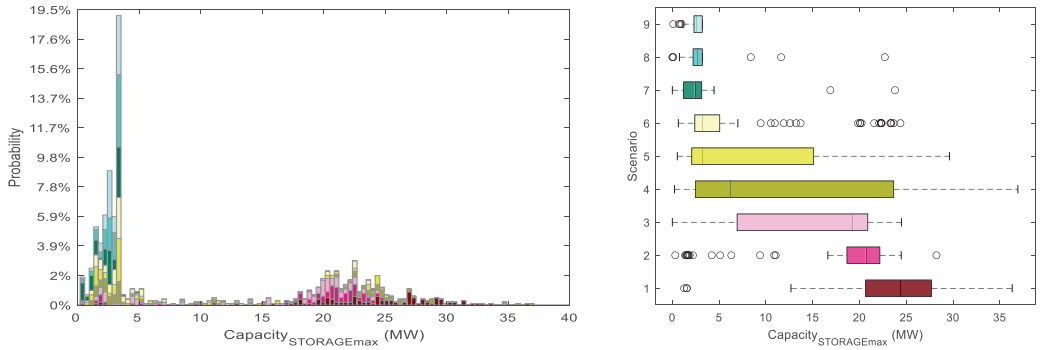

Color	Electricity price	Grid connection peak power cost	Storage capacity (MWh) min	mean	max	Share of data
	low	low	1.3	23.9	36.3	11 %
		medium	0.3	18.5	28.2	10 %
		high	0.0	15.2	24.5	12 %
	medium	low	0.2	12.7	36.9	11 %
		medium	0.5	8.4	29.6	11 %
		high	0.6	6.3	24.4	11 %
	high	low	0.0	2.4	23.8	11 %
		medium	0.0	2.8	22.7	12 %
		high	0.1	2.6	3.2	10 %

Figure 7: Thermal energy storage capacity.

https://doi.org/10.52202/077185-0047

The optimal TES capacity (Fig.7) is centered around two points: below 5 MWh, and 20-25 MWh. The first one consists of mostly medium or high electricity prices, while the second consists mostly of low ones. This indicates two different operation strategies for TES, potentially the first one charging mainly with BB, and the second one with EB. Two main occasions to charge with BB are (i) heat demand drops below BB minimum load during the summer and (ii) heat demand varies over and below maximum BB capacity. For both, the charging and discharging rates are small, supporting smaller TES. In contrast, electric heating could benefit from larger TES to utilize cheap electricity better.

3.2 Clean sheet case

The results for the case where all production capacity except for the LFO boiler had to be invested in were broadly similar to the above-described results for the case of pre-existing 3.5 MW biomass boiler. LCOH variation range increased only slightly, to approximately 82 €/MWh at the high end. Installed heat pump capacities followed a very similar pattern to the case of pre-existing biomass boiler: HP capacities remained at zero in slightly over half the cases. Slightly more capacity was installed at the highest end of the scale, at 1.05 MW_{el} as opposed to just under 1 MW_{el} , but the shares of these results remained minuscule. A slightly greater share of cases, albeit still arguably negligible, resulted in approximately 200 kW_{el} capacity installed. This took place when the wood chip price was high, and the HP CAPEX low.

The sizing of the EB (Fig.8) and the TES (Fig.9) show considerably greater changes than the HP. The EB capacity varies within a similar range as with pre-existing biomass boiler (see Figs 6 and 8), and the peaks are also similarly located at 1, 3, and 5 MW, but without the pre-existing BB the 5 MW peak grows considerably, the 1 MW peak shrinks, and the 3 MW peak all but disappears. Electricity price and grid connection peak power cost remain the most influential uncertainties.

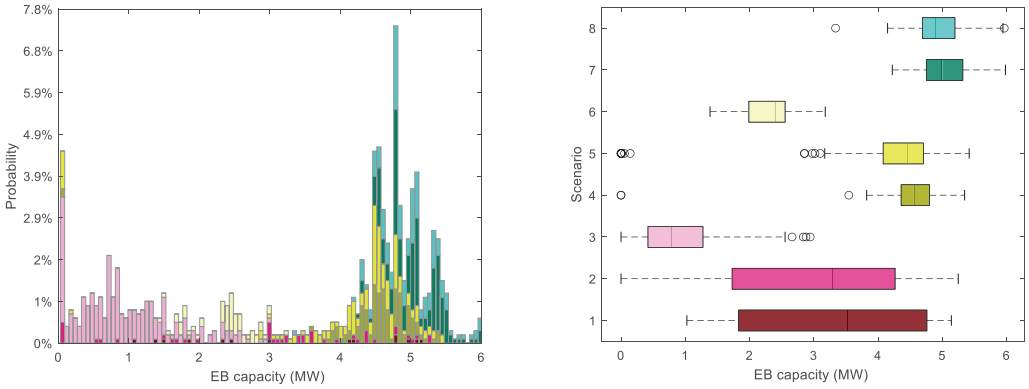

Color	TES capacity	BB capacity	EB capacity (MW) min	EB capacity (MW) mean	EB capacity (MW) max	Share of data
	low	low	1.02	3.30	5.14	1 %
		medium	0.00	2.97	5.25	4 %
		high	0.00	0.91	2.94	28 %
	medium	low	0.00	4.50	5.35	12 %
		medium	0.00	4.12	5.42	15 %
		high	1.39	2.32	3.18	6 %
	high	low	4.22	4.99	5.98	20 %
		medium	3.34	4.93	5.97	14 %
		high	-	-	-	-

Figure 8: Electric boiler (EB) capacity with clean sheet case.

The Fig.8 plot was generated by including the optimized decision variables (installed capacities) as input parameters. This provides insight into how the optimizer is using the electric boiler and the TES in conjunction with each other: TES capacity is the most influential parameter explaining EB capacity, with a large TES corresponding to a large EB, and vice versa. A large TES allows the operation

https://doi.org/10.52202/077185-0047

optimization to use a large EB to make maximum use of the hours of cheap electricity. The second most influential parameter is the BB capacity; large BB is found with small TES and EB, and vice versa. There are no results with large TES, EB, and BB, and only 1% have small TES, EB and BB.

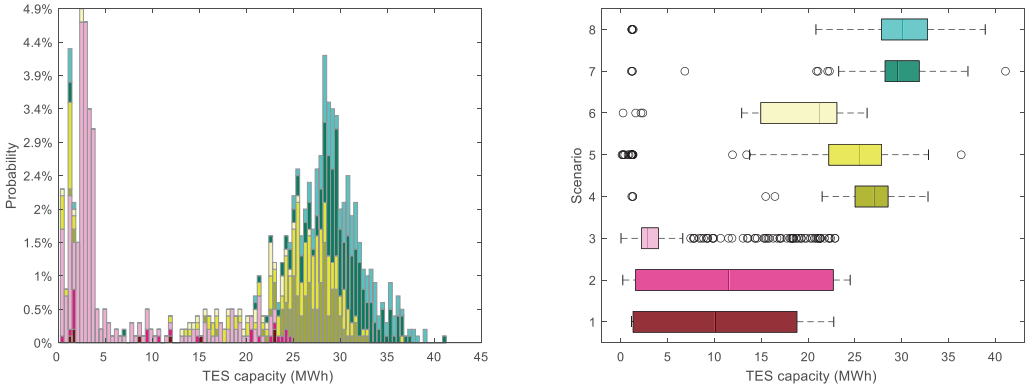

Color	EB capacity	BB capacity	TES capacity (MWh)			Share of data
			min	mean	max	
	low	low	1	11	23	1 %
		medium	0	13	24	2 %
		high	0	5	23	30 %
	medium	low	1	26	33	13 %
		medium	0	23	36	18 %
		high	0	18	26	3 %
	high	low	1	29	41	20 %
		medium	1	29	39	13 %
		high	-	-	-	-

Figure 9: Thermal energy storage (TES) capacity with clean sheet case.

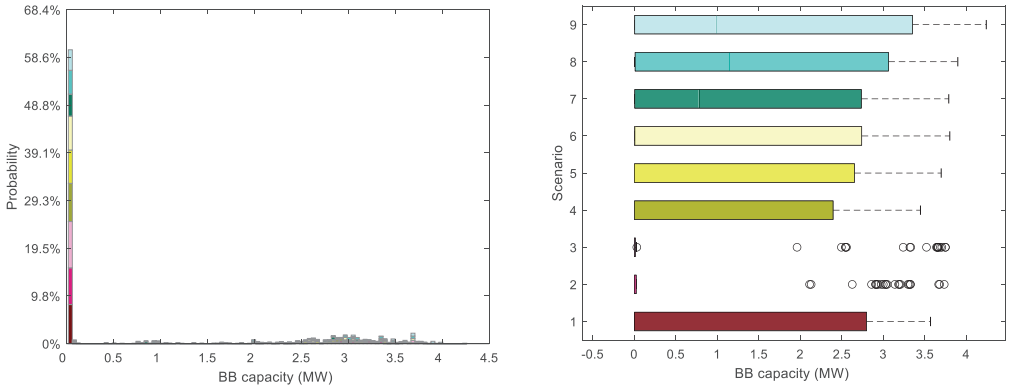

Color	HP capacity	LFO price	BB capacity (MW)			Share of data
			min	mean	max	
	low	low	0.00	1.00	3.57	12 %
		medium	0.00	0.73	3.73	10 %
		high	0.00	0.52	3.75	11 %
	medium	low	0.00	0.78	3.45	11 %
		medium	0.00	1.03	3.70	11 %
		high	0.00	1.17	3.80	12 %
	high	low	0.00	1.24	3.79	10 %
		medium	0.00	1.56	3.90	13 %
		high	0.00	1.60	4.24	10 %

Figure 10: Biomass boiler (BB) capacity.

https://doi.org/10.52202/077185-0047

The TES capacities are similar to the case of pre-existing BB, but with a greater 30 MWh and smaller near-zero peak, largely mirroring the results for EB. The BB data (Fig.10), on the other hand, shows HP capacity and LFO price as the most influential explanations for installed biomass capacity, and a distribution similar to HP. This indicates that the biomass capacity appears to compete with heat pumps for base load in a small number of cases (2.5 to 4 MW installed capacity), as well as oil for peak-load generation.

4 CONCLUSIONS

The combination of electric boiler and TES looks best for base/mid-load district heat generation in all but a small minority of cases, and is superior to air-source heat pumps for taking advantage of low-cost electricity together with TES. It should be noted that this conclusion is limited to the case of air source, and cold climate; if higher temperature heat sources are available, either due to warmer climate, or alternative heat sources, the COP and time within operational limits will support the air-source heat pump, improving economic performance. Biomass boiler and air-source heat pump appear as competing technologies. If the wood chip fuel is cheap, it tends to push out even the small air-source heat pump capacities. For future work, a unit of combined heat and power could be added to represent a larger district heat network.

REFERENCES

Bioenergia, 2023. Bioenergy Association annual report 2023. (In Finnish: Bioenergia ry vuosijulkaisu 2023).

Dahash, A., Ochs, F. and Tosatto A., 2021. Techno-economic and exergy analysis of tank and pit thermal energy storage for renewables district heating systems. *Renewable Energy*, 180, pp.1358-1379.

Dahl, M., Brun, A. and Andersen G.B., 2019. Cost sensitivity of optimal sector-coupled district heating production systems. *Energy*, 166, pp.624-636

David, A., Mathiesen, B.V., Averfalk, H., Werner, S. and Lund, H., 2017. Heat roadmap Europe: large-scale electric heat pumps in district heating systems. *Energies*, 10(4), p.578.

Dorotić, H., Pukšec, T. and Duić, N., 2019. Multi-objective optimization of district heating and cooling systems for a one-year time horizon. *Energy*, 169, pp.319-328.

Fischer, D., Lindberg, K.B., Madani, H. and Wittwer, C., 2016. Impact of PV and variable prices on optimal system sizing for heat pumps and thermal storage. *Energy and Buildings*, 128, pp.723-733.

Hooke, R. and Jeeves, T.A., 1961. "Direct Search" Solution of Numerical and Statistical Problems. *Journal of the ACM (JACM)*, *8*(2), pp.212-229.

Hutty, T.D., Patel, N., Dong, S. and Brown, S., 2020. Can thermal storage assist with the electrification of heat through peak shaving? *Energy Reports*, 6, pp.124-131.

IEA, 2019. Renewables 2019. URL https://www.iea.org/reports/renewables-2019/heat

Immonen, J., and Powell, K.M., 2022. Dynamic optimization with flexible heat integration of a solar parabolic trough collector plant with thermal energy storage used for industrial process heat. *Energy Conversion and Management*, 267, p.115921.

Jaatinen-Värri, A., Honkatukia, J., Uusitalo, A. and Turunen-Saaresti, T., 2024. Centrifugal compressor design for high-temperature heat pumps. *App Therm Eng*, 239, p.122087.

Jain, S.K. and Singh, V.P., 2023. Water resources systems planning and management. Elsevier.

Koskelainen, L., Saarela, R. and Sipilä, K., 2006. *Handbook of district heating* (In Finnish: *Kaukolämmön käsikirja*.) Energiateollisuus.

Kozlova, M. & Yeomans, J.S., 2022. Monte Carlo Enhancement via Simulation Decomposition: A Must-Have Inclusion for Many Disciplines. *INFORMS Transactions on Education* 22, pp.147-159.

Kozlova, M., Ahola, A., Roy, P.T. and Yeomans, J.S., 2023. Simple binning algorithm and SimDec visualization for comprehensive sensitivity analysis of complex computational models. *arXiv preprint arXiv:2310.13446*.

Kozlova, M., Moss, R.J., Yeomans, J.S. and Caers, J., 2024. Uncovering heterogeneous effects in computational models for sustainable decision-making. *Environmental Modelling & Software*, *171*, p.105898.

https://doi.org/10.52202/077185-0047

Krützfeldt, H., Vering, C., Mehrfeld, P. and Müller, D., 2021. MILP design optimization of heat pump systems in German residential buildings. *Energy and Buildings*, 249, p.111204.
Lappeenrannan Energia Oy, 2022. Electricity grid service price catalogue (in Finnish: Sähkön verkkopalveluhinnasto). URL https://www.lappeenrannanenergia.fi/hinnastot-jaehdot/sahkon-verkkopalveluhinnasto
Li, M., Du, W. and Nian, F., 2014. An adaptive particle swarm optimization algorithm based on directed weighted complex network. *Mathematical problems in engineering*, 2014.
Montero, L., Bello, A. and Reneses, J., 2022. A review on the unit commitment problem: Approaches, techniques, and resolution methods. *Energies*, 15(4), p.1296.
Nord Pool, 2022. Historical Market Data. URL https://www.nordpoolgroup.com/en/Market-data1/datadownloads/historical-market-data2
Pieper, H., Ommen, T., Buhler, F., Paaske B.L., Elmegaard, B. and Markussen, W.B., 2018. Allocation of investment costs for large-scale heat pumps supplying district heating. *Energy Procedia*, 147, pp.358-367.
Rinaldi, A., Yilmaz, S., Patel, M.K. and Parra, D., 2022. What adds more flexibility? An energy system analysis of storage, demand-side response, heating electrification, and distribution reinforcement. *Renewable and Sustainable Energy Reviews*, 167, p.112696.
Saari, J., Martinez, C.M., Kaikko, J., Sermyagina, E., Mankonen, A. and Vakkilainen, E., 2022. Techno-economic optimization of a district heat condenser in a small cogeneration plant with a novel greedy cuckoo search. *Energy*, 239, p.122622.
Saltelli, A., Aleksankina, K., Becker, W., Fennell, P., Ferretti, F., Holst, N., Li, S. and Wu, Q., 2019. Why so many published sensitivity analyses are false: A systematic review of sensitivity analysis practices. *Environmental modelling & software*, 114, pp.29-39.
Siddiqui, S., Macadam, J. and Barrett, M., 2021. The operation of district heating with heat pumps and thermal energy storage in a zero-emission scenario. *Energy Reports*, 7, pp.176-183.
Statistics Finland, 2024. Fuel prices in electricity production, most important fuels. [Online] Available: https://pxdata.stat.fi/PxWeb/pxweb/en/StatFin/StatFin__ehi/statfin_ehi_pxt_13p7.px
Tarantola, S., Ferretti, F., Piano, S.L., Kozlova, M., Lachi, A., Rosati, R., Puy, A., Roy, P., Vannucci, G., Kuc-Czarnecka, M. and Saltelli, A., 2024. An annotated timeline of sensitivity analysis. *Environmental Modelling & Software*, p.105977.
Tarragona, J., Pisello, A.L., Fernández, C., de Gracia, A. and Cabeza, L.F., 2021. Systematic review on model predictive control strategies applied to active thermal energy storage systems. *Renewable and Sustainable Energy Reviews*, 149, p.111385.
Tarragona, J., Pisello, A.L., Fernández, C., Cabeza, L.F., Payá, J., Marchante-Avellaneda, J. and de Gracia, A., 2022. Analysis of thermal energy storage tanks and PV panels combinations in different buildings controlled through model predictive control. *Energy*, 239, p.122201.
Trevisan, S., Buchbjerg, B. and Guedez, R., 2022. Power-to-heat for the industrial sector: Techno-economic assessment of a molten salt-based solution. *Energy Conversion and Management*, 272, p. 116362.
Urbanucci, L., D'Ettorre, F. and Testi, D., 2019. A comprehensive methodology for the integrated optimal sizing and operation of cogeneration systems with thermal energy storage. *Energies*, 12(5), p.875.
Wen, L., Suomalainen, K., Sharp, B., Yi, M. and Sheng, M.S., 2022. Impact of wind-hydro dynamics on electricity price: A seasonal spatial econometric analysis. *Energy*, 238, p.122076.
Wu, D. and Ma, X., 2021. Modeling and optimization methods for controlling and sizing grid-connected energy storage: A review. *Curr. Sustain./Renew. Energy Rep*., 8, pp.123-130.
Zhang, Y., Campana, P.E., Yang, Y., Stridh, B., Lundblad, A. and Yan, J., 2018. Energy flexibility from the consumer: Integrating local electricity and heat supplies in a building. *Applied Energy*, 223, pp.430-442.

ACKNOWLEDGEMENT

Authors acknowledge the support by Business Finland under the project 'NEXTHEPS - Development of Next Generation Large Scale Heat Pump Systems (grant number: 1535/31/2022)'.

https://doi.org/10.52202/077185-0047